The Added-Value of Remotely-Sensed Soil Moisture Data for Agricultural Drought Detection in Argentina

M. Mercedes Salvia, *Member, IEEE*, Nilda Sánchez, María Piles, *Senior Member, IEEE*, Romina C. Ruscica, Ángel González-Zamora, Esteban Roitberg, and José Martínez-Fernández

***Abstract*—In countries where the economy relies mostly on agricultural-livestock activities, such as Argentina, droughts cause significant economic losses. Currently, the most-used drought indices by the Argentinian National Meteorological and Hydrological Services are based on field precipitation data, such as the standardized precipitation index (SPI) and the standardized precipitation evapotranspiration index (SPEI). In this article, we explored the performance of the satellite-based soil moisture agricultural drought index (SMADI) for agricultural drought detection in Argentina during 2010-2015, and compared it with the one from the standardized soil moisture anomalies (SSMA), SPI and SPEI (at one-month and three-month temporal scales), using the Agricultural Ministry's drought emergency database as a benchmark. The performances were analyzed in terms of the suitability of each index to be included in an early warning system for agricultural droughts, including true positive rate (TPR), and both false positive and false negative rates. In our experiments, SMADI showed the best overall performance, with the highest TPR and F1-score, and the second best false positive rate (FPR), positive predictive value, and overall accuracy. SMADI also showed the largest difference between TPR and FPR. SSMA showed the lowest FPR, but also the lowest TPR, making it not useful for an alert system. Furthermore, field precipitation-based indices, yet simple and widely used, showed not to be suitable indicators for detection of agricultural drought for Argentina, neither in the one-month nor in the three-month scale.**

***Index Terms*—Agricultural drought detection, Argentina, soil moisture agricultural drought index (SMADI), standardized precipitation evapotranspiration index (SPEI), standardized precipitation index (SPI), standardized soil moisture anomalies (SSMA).**

Manuscript received January 15, 2021; revised March 10, 2021 and May 3, 2021; accepted May 18, 2021. Date of publication May 28, 2021; date of current version July 14, 2021. This work was supported in part by Argentinean Agencia Nacional de Promoción Científica y Tecnológica project PICT 2017-1406, in part by the Spanish Ministry of Science, Innovation and Universities and the European Regional Development Fund under Projects ESP2017-89463-C3-3-R and RTI2018-096765-A-100, and in part by the project Unidad de Excelencia CLU-2018-04 co-funded by ERDF and Castilla y León Government. *(Corresponding author: M. Mercedes Salvia.)*

M. Mercedes Salvia and Esteban Roitberg are with the Grupo de Teledetección Cuantitativa, Instituto de Astronomía y Física del Espacio (IAFE, UBA/CONICET), Ciudad Autónoma de Buenos Aires C1428EGA, Argentina, and also with the Consejo Nacional de Investigaciones Científicas y Técnicas, Ciudad Autónoma de Buenos Aires C1425FQB, Argentina (e-mail: msalvia@iafe.uba.ar; eroitberg@iafe.uba.ar).

Nilda Sánchez, Ángel González-Zamora, and José Martínez-Fernández are with the Instituto Hispano Luso de Investigaciones Agrarias, University of Salamanca, 37185 Salamanca, Spain (e-mail: nilda@usal.es; aglezzamora@usal.es; jmf@usal.es).

María Piles is with the Image Processing Laboratory, Universitat de València, 46980 Valencia, Spain (e-mail: maria.piles@uv.es).

Romina C. Ruscica is with the Universidad de Buenos Aires, Facultad de Ciencias Exactas y Naturales, Ciudad Autónoma de Buenos Aires C1428EGA, Argentina, and also with CONICET–Universidad de Buenos Aires, Centro de Investigaciones del Mar y la Atmósfera (CIMA), Ciudad Autónoma de Buenos Aires C1428EGA, Argentina and also with CNRS–IRD–CONICET–UBA, Instituto Franco-Argentino para el Estudio del Clima y sus Impactos (UMI 3351 IFAECI), Ciudad Autónoma de Buenos Aires, C1428EGA, Argentina (e-mail: ruscica@cima.fcen.uba.ar).

Digital Object Identifier 10.1109/JSTARS.2021.3084849

I. Introduction

In THE last decades, the occurrence and intensity of drought events are increasing and attributable to a decreased precipitation and an increased evapotranspiration driven by global warming [1], [2], with direct and indirect impacts on the economy, environment and food security [3], [4]. Droughts are slow-moving critical hazards with a large time and spatial extension, different from other shorter and more local natural hazards (e.g., floods, hail storms).

There are distinct categories of drought, according to their timescale and on which part of the system suffers from water deficit [5], [6]: meteorological drought, which is associated with a deficit in precipitation, agricultural drought [also known as soil moisture (SM) drought] related with a shortage of water in the soil unsaturated zone that could compromise the crop yields, hydrological drought, that occurs when there is a low water supply in streams, reservoirs, and groundwater levels, usually after many months of meteorological drought; and socioeconomic drought proclaimed when water scarcity leads to unfavorable, and sometimes irreversible, social and economic consequences.

In countries where the regional economy relies mostly on agricultural-livestock activities, such as Argentina, climate variability, particularly droughts, causes significant economic losses [7]–[9]. The drought impact on health is even worse over malnourished and dehydrated populations [10]. Therefore, in order to best mitigate its effects, it is crucial to improve detection, monitoring, characterization, and forecasting of drought events, together with regional decision-making policies (such as the Centro Regional del Clima para el Sur de América del Sur, CRC-SAS; [11]–[15]).

The urgency for identifying severity, location, duration, onset, and cessation of such extreme events have led the world meteorological organization and the global water partnership to create a handbook with the definition of up to 50 drought indicator/indices based on modeled and/or satellite-derived datasets of precipitation, temperature, vegetation, and soil water conditions, among others [16]. The user's choice will depend on the "ease of use," application, available information and computer resources [16] as well as the required temporal and spatial scale (continental, national, and regional). An interesting and relevant observation is that none of the satellite-based indices defined in that handbook includes SM information.

In particular, the most-used drought indices in Argentinian national meteorological and hydrological services are based only on precipitation data from rain gauges [17], [16], such as the standardized precipitation index (SPI, [18]), or at most they include the role of temperature, as the standardized precipitation evapotranspiration index (SPEI, [19]). Examples of the use of these indices in Argentina can be found in [20] and [21].

Since a precipitation deficit propagates through the system into (potentially) SM and streamflow anomalies, drought types are inherently related. Probably for this reason, together with the fact that there is a wider availability of ground-based stations measuring precipitation than measuring SM, precipitation-based indices are typically used for the detection of agricultural drought. However, the processes involved in the evolution of droughts are complex [22], especially over agroecosystems, where the deficit in plant-available water that could compromise crop production depends on the type of crop, its location, and season of the year. Hence, precipitation-based indices, yet simple and widely used, may not be the most suitable indicators for detecting agricultural drought.

Alternatively, the use of remote sensing data for drought detection has been historically based on water and temperature–related vegetation stress indicators, particularly the vegetation condition index (VCI) and temperature condition index (TCI), respectively. Examples of its use in Argentina can be found in [23]–[25].

More recently, satellite-based (surface) SM estimates have been used for detection and description of agricultural droughts in Argentina [26], [27] and worldwide [28], [29], [30]. Nonetheless, satellite products used in those studies provide information on the moisture of only the topsoil layer (approximately 5 cm in the best case) and not the root zone layer, where agricultural droughts are usually defined. Undoubtedly, global satellite-based surface SM data provides valuable information for the study of droughts, yet it is important to remark that it offers only an indirect link to the processes involved. Root zone SM products based on assimilation or vertical propagation of surface satellite data have recently been made available (SMAP L4, SMOS L4), and their use for drought assessment has been also suggested in recent studies [31]–[33].

As an alternative to the use of a single variable to characterize droughts, Sánchez *et al.* [34] proposed the soil moisture agricultural drought index (SMADI) to integrate into a single indicator the combined effects of SM deficit, high temperatures, and vegetation stress. It is based solely on remote sensing datasets of surface SM, land surface temperature (LST), and normalized difference vegetation index (NDVI). Its formulation imposes a delayed impact of drought in vegetation status with respect to surface conditions, resulting in a greater capacity for early detection of droughts [35]. Several studies have shown a reasonable match of SMADI with other climatic-agricultural indices and with registered events of drought at regional [35], [36] and global scales [37]. However, its performance has not yet been evaluated for the distinct socioeconomic and agroecological conditions of Argentina.

Furthermore, most of the previous works assessing SMADI and/or other drought indices performance are based solely in their detection percentages. This means they are taking into account only how the analyzed indices perform during what are considered to be real drought events, but they do not take into account how those indices behave during normal or wet periods. This latter kind of analysis is extremely important if the purpose of the evaluation is assessing the suitability of the index not only to describe/analyze droughts events, but also for drought detection through an early warning system. In order to be trustworthy and useful, decision support systems should have good detection capabilities of real drought events, but also not raise many false drought alarms over normal or wet periods.

In this line, the main goal of this research is to explore the performance of SMADI for agricultural-socioeconomic drought detection and monitoring in Argentina. The secondary goal is to compare the SMADI performance with standardized soil moisture anomalies (SSMA), SPI and SPEI, in the detection of agricultural drought emergencies declared in Argentina in the last years. For this, the Argentina's Ministry for Agriculture emergencies database [38] was used as a benchmark, and the period of study spanned from June 2010 to December 2015. The obtained results are analyzed in terms of the suitability of each index to be included in an early warning system for agricultural droughts.

II. Study Area

Argentina is located in the southernmost part of the American Continent. It has a continental surface of 2 791 810 km² and expands from 21° 46′ 52″ S to 55° 03′ 21″ S, and 53° 38′ 15″ W to 73° 34′ W [39]. The Country is geopolitically composed of 24 provinces that are internally divided into departments.

North of 40° S, the climate is subtropical with warm summers, and annual mean temperatures span from 14 °C to 22 °C [40], [41]. Across these latitudes, water vapor sources are the Atlantic Ocean and the continental tropics since the Andes Mountains to the west act as a barrier to the entry of humid air from the Pacific [42]. Consequently, a dry-to-wet gradient from SW to NE is quite representative of the precipitation in the region, ranging from 100 mm to more than 1200 mm mean annual precipitation [40], [42]. South of 40° S, the Patagonia climate is cool-temperate and windy. The Pacific westerly winds drop their moisture over the southern Argentinian Andes in a narrow band of western Patagonia, and as a consequence, the rest of Patagonia is dry with annual precipitations below 200 mm [41], [43].

Argentina's agricultural activities are almost exclusively rainfed, with less than 1.4 Million hectares of irrigated agriculture, according to the last National Agricultural Census [44]. The five most extended crops are soybean, corn, wheat, sunflower, and oat, in that order, and they account for almost 90% of the sowed area. Argentina's agricultural production can represent up to 10% of gross domestic product and reach a share of 55% of total exports [8], [45]. In this line, the income loss of soybean production due to drought events in 2016 was of $8046 million dollars, equivalent to 22% of Argentinean international reserves of that year, and drought events for 2018 led to a decrease of $2871 million dollars, nearly 0.5% of gross domestic product [9], [45]. As an example of the temporal characteristics of the agricultural activity in Argentina, Table I gives sowing and harvesting times for the ten most extended crops in the country

TABLE I
GROWING STAGES FOR THE TEN MOST EXTENDED CROPS OF ARGENTINA (FROM JULY TO JUNE)

	J	A	S	O	N	D	J	F	M	A	M	J
Soybean				░	░	░			█	█	█	
Corn			░	░						█	█	█
Wheat	░				█	█	█				░	░
Sunflower	░	░	░	░	░	█	█	█	█			
Oats					█	█		░	░	░	░	░
Barley	░				█	█					░	░
Sorghum				░	░	░		█	█	█	█	
Cotton				░	░	░			█	█	█	█
Peanut			░	░	░	░			█	█		
Rye				█	█	█	█	░	░	░	░	░

Sowing period ░ Harvesting period █

TABLE II
DROUGHT CATEGORIES FOR THE ANALYZED INDICES

	SMADI	SSMA	SPI	SPEI
Normal or wet	< 1	> -1	> -1	> -1
Mild drought	1 to 1.99			
Moderate drought	2 to 2.99	-1 to -1.49	-1 to -1.49	-1 to -1.49
Severe drought	3 to 3.99	-1.5 to -1.99	-1.5 to -1.99	-1.5 to -1.99
Extreme drought	≥ 4	≤ -2	≤ -2	≤ -2

for the 2018–2019 campaign, accounting for 97,6% of the sowed area [46],[47]. Data are shown on a monthly basis to account for the temporal variability of local conditions due to the large extension of Argentina's agricultural area, both between and within provinces. For instance, sunflower's sowing time is July/August for the provinces of Chaco and Formosa, October/November for the provinces of Buenos Aires, La Pampa and San Luis, and ranges from July to October for the different departments of Santa Fe province. We can see that 6 of the 10 most extended crops (soybean, corn, sunflower, sorghum, cotton and peanut) are summer crops (i.e., sowed during austral spring and harvested in austral autumn, after growing throughout austral summer). These six crops account for 74% of the total sowed area. The remaining four crops are winter crops (wheat, oats, barley and rye) and comprise 23.6% of the total sowed area.

III. Data and Methods

As stated in the introduction, one of our objectives is to evaluate the SMADI index for agricultural drought detection in Argentina and to compare its performance with other well-known drought indices. For this purpose, the agricultural drought emergencies declared by the Ministry for Agriculture were used as benchmarks. The following sections introduce the analyzed indices, the methodology followed to define drought and non-drought events from the agricultural emergency declarations, and the performance metrics used for validation as well as for assessing the suitability of the indices for inclusion in an early warning system.

A. Indices

1) Soil Moisture Agricultural Drought Index: This novel index, presented in an application over the Iberian Peninsula for the first time by [34], leverages from the increasing number of remote sensing databases (e.g., SM from passive microwave sensors, LST and VI from optical sensors) available at a variety of spatial scales and temporal ranges. The index is based solely on remote sensing sources, and it is scalable both in space and time (depending on the selected input data). The core of its rationale is the inclusion of SM to focus on agricultural drought. SMADI coupled two well-known advances about the SM applications using remotely-sensed datasets. First, the inverse relationship found between the soil skin temperature (using the LST as a proxy of this parameter in SMADI) and the vegetation status (using the NDVI), both of which are in turn closely related to SM [48]. This relationship is known as the "Universal Triangle," from the relationship obtained between LST and NDVI with SM when plotted in a two-dimensional scatterplot, and has been applied in numerous studies dealing with retrievals of SM and evapotranspiration [49]–[51]. Second, this relationship, expressed as a regression formula in which SM is the target variable, has also allowed for the improvement of the spatial resolution of coarse SM passive microwave products using higher spatial resolution LST and NDVI data [52]–[54].

Therefore, SMADI accounts for the LST/NDVI slope and the SM in the form (1)

$$\mathrm{SMADI}_i = \mathrm{SMCI}_i \frac{\mathrm{MTCI}_i}{\mathrm{VCI}_{i+1}} \tag{1}$$

where SMCI, MTCI, and VCI are the normalized SM, LST, and NDVI, respectively, using the maximum and the minimum time range values for each, following the form of Condition Index of [55], [56], with minor modifications

$$\mathrm{VCI} = \frac{(\mathrm{NDVI}_i - \mathrm{NDVI}_{\min})}{(\mathrm{NDVI}_{\max} - \mathrm{NDVI}_{\min})} \tag{2}$$

$$\mathrm{MTCI} = \frac{(\mathrm{LST}_i - \mathrm{LST}_{\min})}{(\mathrm{LST}_{\max} - \mathrm{LST}_{\min})} \tag{3}$$

$$\mathrm{SMCI} = \frac{(\mathrm{SM}_{\max} - \mathrm{SM}_i)}{(\mathrm{SM}_{\max} - \mathrm{SM}_{\min})} \tag{4}$$

where *i* corresponds to the selected temporal period (two weeks, in this case). Notice that in (1), VCI was calculated for $i+1$, i.e., with a time lag of fourteen days as regards to SMCI and MTCI, since it is expected that the effect that temperature and humidity have on surface conditions appears later in plants [57], [58]. The SMADI values are then classified into five drought intensity categories, following [37] (see Table II).

For this article, SMADI has been computed pixel-based following (1) at a spatial resolution of 0.05°, through the integration of products MODIS/Terra LST (MOD11C1 v.6), MODIS reflectance (MOD09CMG v.6), and SMOS L3 SM (BEC v2.0, [59]). Daily observations of input products were composited into biweekly time series before computing the index, as in [37]. The global biweekly SMADI product for the period 2010-2015 used in this work is freely available online [60].

2) ESA-CCI Standardized Soil Moisture Anomaly: To calculate the SSMA (5), the ESA-CCI SM Combined product from the ESA's CCI suite of essential climate variables was used. The CCI goal is to produce a complete and consistent global SM data record based on passive (radiometer) products, active (radar/scatterometer) products, and a combination of both. The CCI-SMv04.7 COMBINED is available from 1979 to 2019 at 0.25° spatial resolution and daily temporal resolution (http://www.esa-soilmoisture-cci.org, [61]–[63])

$$\mathrm{SSMA}_i = \frac{\mathrm{SM}_i - \overline{\mathrm{SM}_i}}{\sigma_{\mathrm{SM}_i}} \tag{5}$$

where *i* corresponds to a given biweekly period (same as for SMADI), SM_i is the biweekly average, $\overline{\mathrm{SM}_i}$ is the long term average and σ_{SM_i} is the standard deviation, which are both calculated for the same biweekly period *i*, but including the complete baseline period 1979–2019. Table II provides the classification of SSMA values into four drought intensity categories [64].

3) Standardized Precipitation Index and Standardized Precipitation and Evapotranspiration Index: The SPI [18] quantifies precipitation excess or shortage for a given place and time scale. To this end, precipitation values are converted to probabilities based on long-term precipitation records computed at the chosen time scale. Since precipitation does not follow a Gaussian distribution, a gamma probability model was used to fit the 40-year reference period of precipitation (1971–2010) for the study area [17].

The SPEI [19] follows the same conceptual design as SPI, but considers the role of temperature by adding to the precipitation series the potential evapotranspiration (PET). SPEI involves a climatic soil water balance and the accumulation of deficit/surplus, making it a better agriculture drought index than SPI in a warming climate.

There are different criteria in the literature regarding which temporal scale is the best suited for detecting agricultural droughts. For example, [34] stated that the one-month SPI is generally used to reflect short-term conditions related to short-term SM and crop stress, especially during the growing season. However, [17] stated that two-to-three month scales had well-represented agricultural droughts, and [65] reported that SPI at a three-month scale reflects wet or dry conditions for short and medium time ranges and provides estimates of the climate conditions at critical stages of the crops' growth. Considering this, we decided to employ precipitation-based indices with both one-month (i.e., SPI1, SPEI1) and 3-month (i.e., SPI3, SPEI3) temporal scales.

These precipitation based indices were computed and provided by the Regional Climate Center Network for Southern South America [66] at a spatial resolution of 0.25°. Table II gives the classification of SPI and SPEI values into four drought intensity categories [67]. This classification is the same regardless of index temporal scale.

B. Definition of Drought and Nondrought Events

A drought index should (at least) have two desirable characteristics: it should detect the occurrence of droughts, and it should not falsely detect a drought when there is no real drought event. To analyze these conditions, we distinguish henceforth between actual drought and nondrought events, respectively.

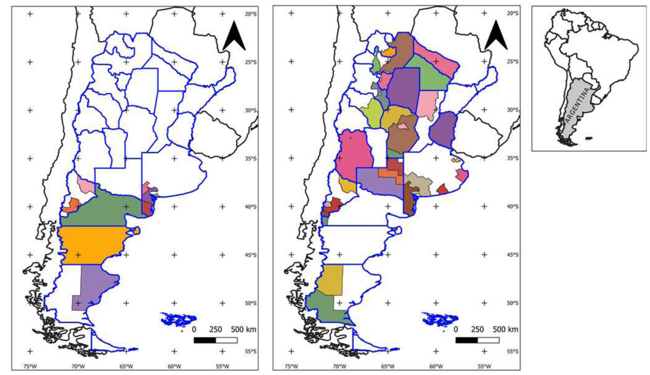

Fig. 1. Actual drought events (left) and nondrought events (right) for 2011–2012. Adjacent areas with different colors correspond to separate events.

Actual Drought Events: We used the agricultural drought emergencies declared by Argentina's Ministry for Agriculture [38] as a benchmark of the actual drought events. These declarations focus on productive areas at the spatial scale of departments (smaller administrative units that exist within each province) and at a temporal scale that usually includes the whole productive cycle affected (even if the drought covered only part of the cycle or continued after the productive cycle had finished). In each department/province, emergencies are often declared within the same production cycle, but only after the drought effects have started to be observed by producers. Given the fact that an emergency declaration implies a tax exemption for producers (reducing tax collection for the State) and that the Ministry can take a significant amount of time to analyze how seriously the productive activities have been affected, it is unlikely for an emergency to be declared without the actual occurrence of drought, which makes these declarations extremely useful as a posteriori ground truth for actual drought events. We downloaded the resolution documents for every emergency declaration for the period between June 2010 and December 2015, and digitized them in time and space, aggregating all departments involved in that particular emergency for each province. This was a three-step process: First, we used a shapefile containing the polygons for each department in Argentina, labeled also according to the province they belong to. In this shapefile we added as attributes the date for the beginning and end of each declared emergency for each involved department. Second, for each emergency declaration we created a new shapefile, with a single polygon that aggregated departments belonging to the same province and having the same dates for the start and end of the emergency. Third, we assigned resulting actual drought events to the year of its starting date, regardless of the ending date of the emergency.

We found a total of 49 actual drought events, 23 starting in 2010–2011, 9 in 2011–2012, 8 in 2012–2013, and 9 in 2013–2014. From July 2014 to December 2015, there was not any declaration of drought emergency. As an example, the spatial extension of actual drought events for years 2011-2012 are illustrated in the left panel of Fig. 1. Austral winter-to-winter annual timescale, starting on July 1st is considered in order to include the growing cycle of most extended crops (summer crops) into a single year definition (see Table I).

Nondrought Events: Nondrought events were defined as the periods between emergency declarations for departments with at least one emergency declared in the studied period. This definition is based on the fact that emergencies are only declared for productive areas, so if a given department did not have any emergency declared, the reason could be that the Ministry does not consider it a productive area and, thus, its drought condition is not evaluated. Alternatively, it could be noted that a given department may be considered as a productive area, its condition being evaluated, but it did not suffer from a drought, or it suffered a drought that was not severe enough to compromise production. But since we cannot discriminate between those three situations, and in order to homogenize the criterion used for the whole study region, we decided not to take into account departments that did not have any declarations for the period 2010–2015. As for the actual drought events, nondrought events were defined at the department scale and then aggregated at the province level and for austral winter-to-winter annual timescales (see Fig. 1, right). In this case, the procedure was as follows: First, for each department included in at least one actual drought event, we registered the time between the start of the study period and the beginning of the first emergency declared, the end of a drought emergency and the beginning of the next, and the end of the last registered drought event and the end of the study period. Then, at the province level, departments that are spatially contiguous and have the same dates of start and end of the nondrought periods are aggregated as a single nondrought event. This resulted in 167 nondrought events (29 for 2010–2011, 31 for 2011–2012, 32 for 2012–2013, 30 for 2013–2014, 23 for 2014–2015, and 22 for July 1 to December 31 2015).

C. Evaluation Strategy

1) Performance Metrics: Following [37], for each spatio-temporal event (actual drought or nondrought), the following metrics have been calculated for each index.

1) *% Positives*: Percentage of events that are considered positive (detected) for any drought category (mild, moderate, severe, extreme).
   a) For SMADI (or SSMA), a positive is considered if there is at least ⅓ of the event area for two consecutive biweekly time steps with a value of SMADI ≥ 1 (or SSMA ≤ -1).
   b) For SPI and SPEI, a positive is considered if there is at least ⅓ of the event area with SPI or SPEI ≤ -1 for any single period (monthly or 3-monthly).
2) *% Duration*: Percentage of time within the event period that is considered a positive for the corresponding index. Informed value is the average of the duration of individual events.
3) *% Extreme*: Percentage of events that are positive and have at least one pixel with an extreme drought category of the corresponding index (SMADI$\geq$ 4, SSMA< -2, SPI< -2, SPEI< -2, Table II).

These three metrics objectively quantify detection capabilities of occurrence (% positives), severity (% extreme) and timing (% duration). While % positives and % extreme are spatial drought detection metrics, % duration is temporal, i.e., the focus is on detecting onset and cessation of drought events.

The three metrics are percentages distinctively computed both on an annual basis and for the whole studied period as a unit. In the latter case (referred to as "total" in all tables showing metrics results), all emergencies were pooled together regardless of the occurrence year, to grant them the same weight in calculations. For this reason, since each year has a different number of events, Total number of events is the sum of the annual number of events, but total % positives and total % extreme are not the average of annual percentages. Instead, Total % positives (or % extreme) is the sum of all the events considered positive (or extreme) throughout the studied period, divided by the total amount of events considered for the whole period (49 for actual drought events, 167 for nondrought events).

For a good performance, it is expected that a drought index would show a high % true positives (positives on actual drought events) and a low % false positives (positives in nondrought events). The same would be expected from % extreme and for % duration (high for actual drought events, low for nondrought events).

For actual drought events, we used an inclusive time schedule. This means that if a given drought event includes only 1 of the 14 days considered within a biweekly time step in the SMADI time series (or SSMA), then such a SMADI biweekly time step is part of that actual drought event time frame. The same criterion was also applied to precipitation-based indices. On the contrary, for nondrought events, we used an exclusive time schedule. This means that a given drought index period is considered part of the nondrought event if it was fully included in the event. Furthermore, given that the ending of actual drought events (and beginning of nondrought events) is defined by the end of the productive cycle even if the drought continues, false positives completely adjacent to drought events were not recorded.

Given the use of polygons with established geographical limits for the definition of events, the "location" characteristic is included in the occurrence of the drought, that is, if for a particular event, an index observes a drought but does not locate it within the event polygon, it is not considered a positive.

2) Early Warning System Suitability Analysis: The importance of drought detection and monitoring for Argentina's economy encourages the development of a drought early warning system, both for the timely declaration of agricultural emergencies and for the mitigation activities. Therefore, in addition to the detection of spatial and temporal drought events we evaluated the suitability of the different analyzed drought indices for their use in an early warning system. To do so, for each of the analyzed indices, we used the absolute number of positive events for actual drought and nondrought events for the whole studied period to construct a 2-by-2 confusion matrix. From this, the following summary statistics were computed and compared (see Table III): the recall or true positive rate (TPR), the fall out or false positive rate (FPR), the precision or positive predictive value (PPV), the F1-score, and the overall accuracy (OA).

TPR and FPR were already explained in the previous section as % true positives and % false positives, and they indicate index ability to detect actual drought (TPR), and how many false alarms we would get by believing in the index results (FPR). PPV shows the relation between true positives and all

TABLE III
CATEGORICAL STATISTICS USED TO COMPARE THE SUITABILITY OF THE DIFFERENT DROUGHT INDICES FOR THEIR INCLUSION IN AN EARLY WARNING SYSTEM

	Equation	Description
True Positive Rate (TPR, recall) (%)	$TPR = \frac{TP}{TP + FN} * 100$	Percentage of actual droughts that were successfully identified as droughts.
False Positive Rate (FPR, fall out) (%)	$FPR = \frac{FP}{FP + TN} * 100$	Percentage of non-droughts that the index identified as drought
Positive Predictive Value (PPV, precision) (%)	$PPV = \frac{TP}{TP + FP} * 100$	Percentage of droughts detected by the index that were actually droughts
F1-score (%)	$F1 = 2 * \frac{TPR * PPV}{TPR + PPV}$	Integration of TPR and PPV through their harmonic mean
Overall Accuracy (OA) (%)	$OA = \frac{TP + TN}{TP + FP + FN + TN} * 100$	Percentage of events that have been correctly classified either as drought or non-drought
TP = True positives; FP = False positives; FN = False negatives (#Actual drought events - TP); TN = True negatives (#Nondrought events - FP).		

detected positives. These three categorical statistics are useful to evaluate the index suitability for their inclusion in an early warning system, but the three should be jointly assessed, since evaluation of only one or two could lead to misleading results, i.e., the perfect index would have a 100% TPR, a 0% FPR, and 100% PPV, but one index can have both a large TPR and a large FPR, and thus a smaller PPV than other index. To synthesize the evaluation scores into a single metric, we also included F1-score and OA. These statistics are widely used in machine learning experiments, medical sciences, behavioral sciences, climate sciences, and remote sensing classification evaluations, amongst others [68]–[70].

OA was included because it is very well known and widely used to evaluate remote sensing classification results and is often considered a benchmark metric for accuracy assessment, based on its computing simplicity and intuitive nature as an accuracy measurement (correctly classified events or pixels over the total analyzed events or pixels). However, this metric is quite sensitive to the prevalence of the classes or studied events, especially for imbalanced binary classifications [71], [72]. Drought detection is one of these cases since droughts have a relatively low prevalence, and in a given period, there are usually more nondrought than drought events. For cases like these, OA assigns more weight to the correct detection of nondrought events than to the correct detection of actual drought events and its errors. On the other hand, F1-score is based on the number of true positives and its relation with the number of errors (false positives for PPV and false negatives for TPR) and ignores the number of true negatives, thus better summarizes the performance of the evaluated indices in terms of their suitability for a drought early-warning system.

IV. RESULTS AND DISCUSSION

A. Detection Capabilities for a Case Study

Series of drought maps for Argentina were derived for each index. As a given example of those maps, Fig. 2 illustrates how the six indices captured the drought emergency declared between July 1 and December 31, 2013 for northern Santa Fe Province (blue polygon).

This emergency was detected as true positive at some point of its six month length by the six indices, and five of them also coincided in at least one of the positive (detected) periods. Regarding the SM-based indices, SMADI showed positives in seven consecutive biweekly time steps (out of the 14 included in the emergency declaration) between July 30 and November 4; and SSMA exhibited positives between August 13 and September 9 (two consecutive biweekly time steps), and between September 24 and October 21 (two consecutive biweekly time steps). Regarding the monthly precipitation-based indices, SPI1 showed a positive only for August, 2013, and SPEI1 revealed positives for August and December 2013. As for three-monthly precipitation based indices SPEI3 showed positives for August and September 2013 and SPI3 displayed a single positive for September 2013. As a result, the indices coincide in the drought detection during August 2013, except SPI3 that detected the emergency in September (with the integration of rainfall data from July, August and September).

This case study exemplifies the influence of the temporal scale used for SPI calculation. The fact that SPI1 showed drought conditions in August means that rainfall was lower than its historical value for that month. However, SPI3 did not show drought conditions for August, which means that in June and July rainfall was enough to compensate for August's deficit. At the same time, neither July nor September showed drought conditions according to SPI1, but when accumulating the shortage of rainfall for the months of July, August and September, SPI3 showed drought conditions.

The evolution in time of the SMADI index on the northern part of Santa Fe province and surroundings for the seven-match sub-periods is analyzed in detail in Fig. 3. As can be seen in Figs. 2 and 3, the drought event seems to extend beyond northern Santa Fe, covering a large part of the center-north of Argentina. In fact, both the provinces to the North and the West of Santa Fe had emergencies declared starting on July 1, 2013, and with different ending dates, which support the obtained maps. Regarding temporal evolution, SMADI shows over a 60% spatial extension of the different classes of drought intensity for over 40% of the time the emergency was declared. Moreover, it showed over 8% extension of extreme drought values for more than 35% of the emergency duration. We can also observe that SMADI extreme drought values are present as continuous areas and not as isolated pixels, providing more confidence in its estimations.

B. Drought Indices Performance

From a statistical point of view, Tables IV–VI show the annual and total number of actual drought and nondrought events with their performance metrics for the SMADI, SSMA, and precipitation-based indices (SPI1, SPEI1, SPI3, and SPEI3), respectively.

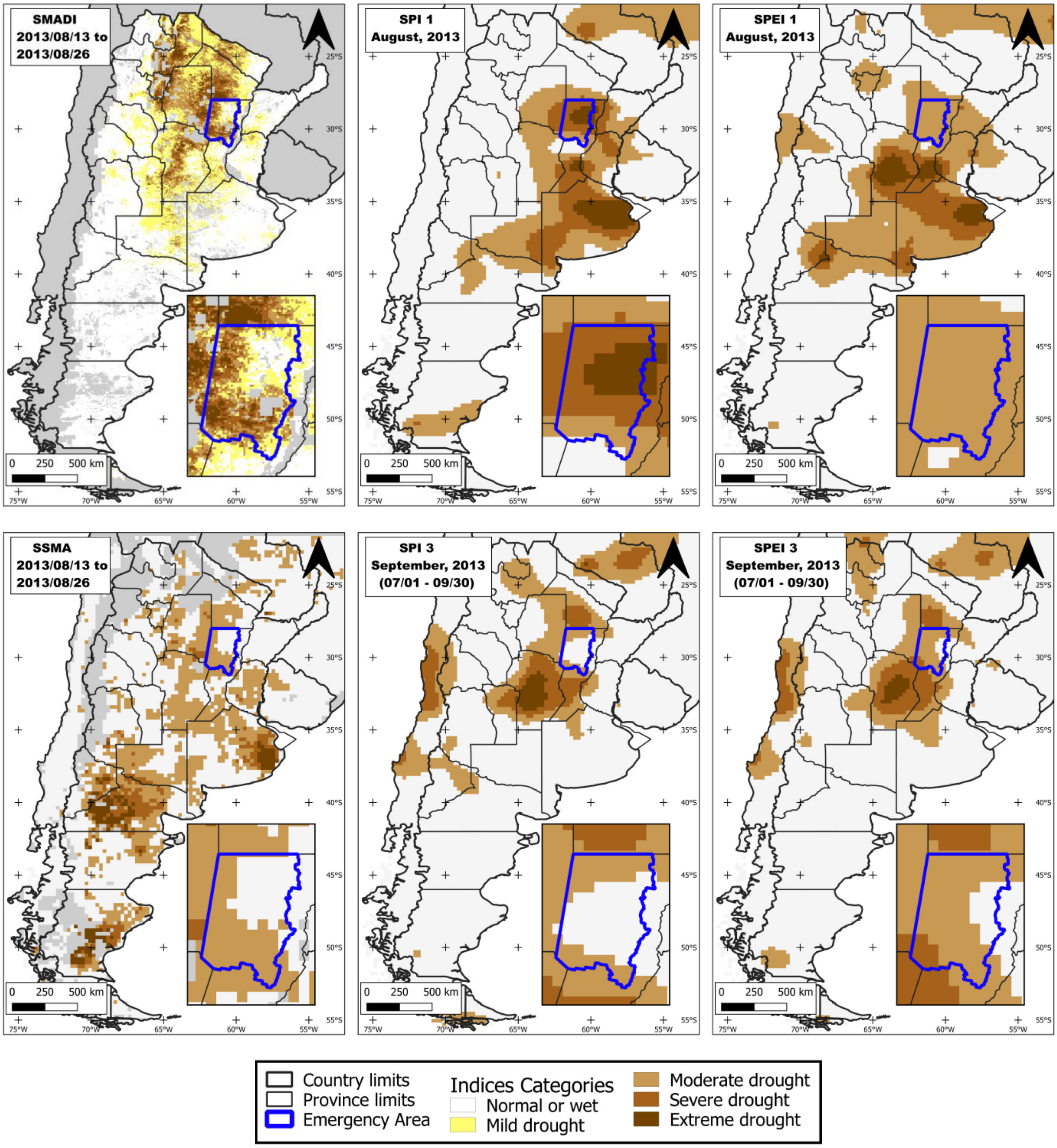

Fig. 2. Spatial patterns of the six drought indices illustrate detection capabilities for the emergency declared between July 1 and December 31, 2013 in Northern Santa Fe province (blue polygon).

TABLE IV
ANNUAL AND TOTAL NUMBER OF ACTUAL DROUGHT AND NONDROUGHT EVENTS AND PERFORMANCE METRICS FOR SMADI. NOTICE NO ACTUAL DROUGHT EVENTS OCCURRED FROM JULY 2014 TO DECEMBER 2015

Index	Events	Actual Drought Events					Nondrought Events						
	Period	2010-11	2011-12	2012-13	2013-14	**TOTAL**	2010-11	2011-12	2012-13	2013-14	2014-15	2015	**TOTAL**
	Number	23	9	8	9	**49**	29	31	32	30	23	22	**167**
SMADI	**% Positives**	78	100	100	67	**84**	52	55	47	53	70	41	**53**
	% Duration	30	29	38	31	**32**	27	27	26	25	17	26	**25**
	% Extreme	65	89	100	67	**76**	41	48	41	37	48	27	**41**

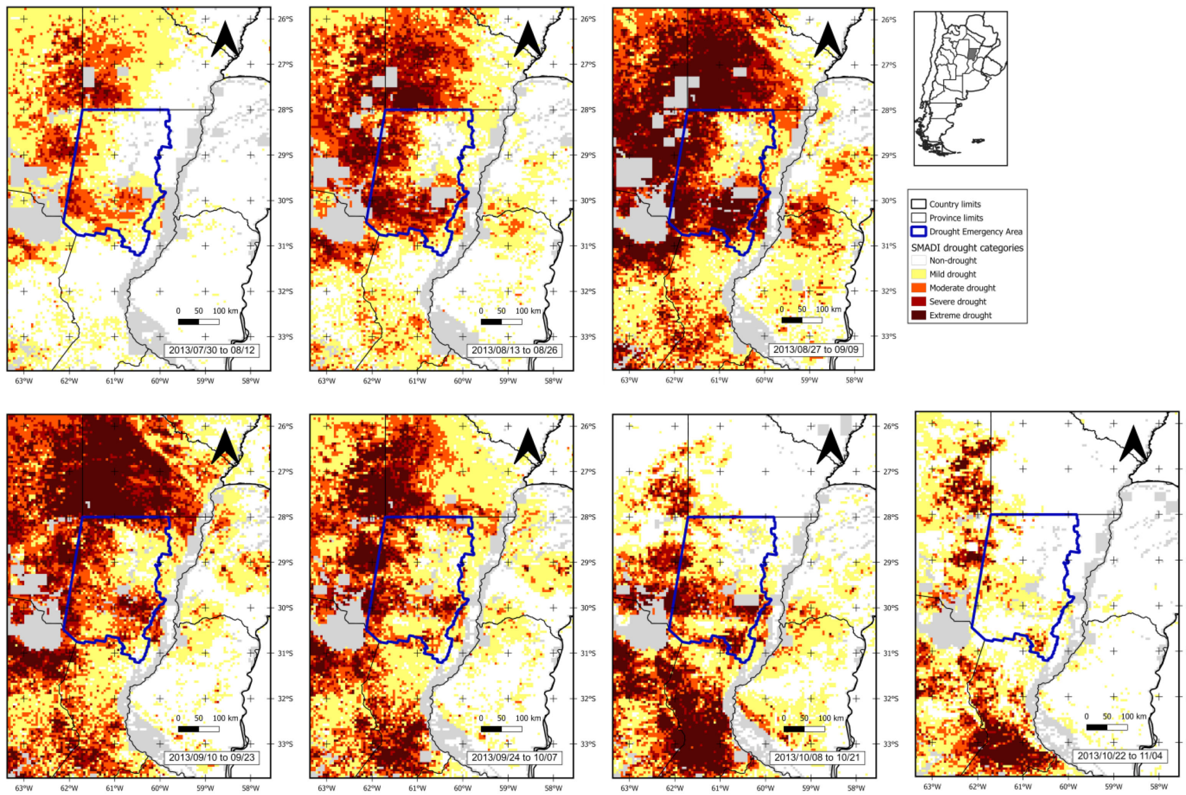

Fig. 3. Temporal evolution of SMADI index for the drought emergency declared between July 1 and December 31, 2013 in northern Santa Fe province (blue polygon). From top left to bottom right are the 7 consecutive biweekly time steps in which SMADI falls into a mild-to-extreme drought category, starting July 30 and ending November 4.

TABLE V
Annual and Total Number of Actual Drought and Nondrought Events and Performance Metrics for SSMA. Notice No Actual Drought Events Occurred From July 2014 to December 2015

Index	Events	**Actual Drought Events**					**Nondrought Events**						
	Period	2010-11	2011-12	2012-13	2013-14	**TOTAL**	2010-11	2011-12	2012-13	2013-14	2014-15	2015	**TOTAL**
	Number	23	9	8	9	**49**	29	31	32	30	23	22	**167**
SSMA	**% Positives**	26	89	75	33	**47**	10	39	41	23	13	9	**24**
	% Duration	18	15	29	10	**19**	23	21	16	12	13	15	**17**
	% Extreme	9	56	25	0	**18**	0	13	22	10	4	5	**10**

Analyzing the whole study period (i.e., total), SMADI allowed for good detection capabilities for actual drought events when considering the spatial extension of different drought classes (84% of Positives). It also showed extreme values in the vast majority of the events (76% of Extreme). In other words, SMADI detected declared emergencies in space and severity with a confidence higher than 75%. SMADI also exhibited outstanding performances at the annual scale, both regarding detection and extremes (over 65% for every year in both metrics). In fact, in 2011–2012 and 2012–2013, SMADI showed perfect detection of declared emergencies, and in 2012–2013 and 2013–2014, all detected emergencies included extreme values.

SMADI results regarding actual drought duration were considerably lower, with an average of 32% of the temporal extent of the emergency declarations detected as drought. This result can partially be explained by the nature of the emergency declarations used as actual events, which determines how their temporal scale is registered. As we mentioned before, the Ministry's goal is to generate tax refunds for affected agricultural producers, and emergencies are declared for the entire affected productive cycle (with a different length for crops, cattle raising, etc.). However, drought duration does not necessarily need to match the productive cycle duration to affect crop yield (e.g., a drought occurring only during crop early growth-developmental stages can have the highest impact). Hence the temporal coverage for

TABLE VI
ANNUAL AND TOTAL NUMBER OF ACTUAL DROUGHT AND NONDROUGHT EVENTS AND PERFORMANCE METRICS FOR SPI1, SPEI1, SPI3 AND SPEI3. NOTICE NO ACTUAL DROUGHT EVENTS OCCURRED FROM JULY 2014 TO DECEMBER 2015

Index	Events	**Actual Drought Events**					**Nondrought Events**						
	Period	2010-11	2011-12	2012-13	2013-14	**TOTAL**	2010-11	2011-12	2012-13	2013-14	2014-15	2015	**TOTAL**
	Number	23	9	8	9	**49**	29	31	32	30	23	22	**167**
SPI1	**% Positives**	83	89	75	44	**76**	66	77	75	47	70	41	**63**
	% Duration	19	16	13	11	**17**	18	21	18	13	15	22	**18**
	% Extreme	35	11	50	44	**35**	24	26	44	20	35	18	**28**
SPEI1	**% Positives**	74	89	100	78	**82**	69	87	87	53	87	36	**71**
	% Duration	22	18	25	19	**21**	17	29	21	21	16	20	**21**
	% Extreme	22	33	50	33	**31**	0	16	25	10	39	0	**15**
SPI3	**% Positives**	52	78	100	56	**65**	66	77	66	40	57	41	**59**
	% Duration	23	28	37	19	**27**	21	24	25	17	15	20	**22**
	% Extreme	30	44	100	33	**45**	17	32	31	27	26	23	**26**
SPEI3	**% Positives**	61	100	100	56	**73**	66	81	69	50	96	36	**66**
	% Duration	27	28	46	23	**31**	19	28	26	19	19	21	**23**
	% Extreme	35	33	62	11	**41**	17	32	31	30	35	27	**29**

a drought is usually overestimated in the emergency declarations (as in the six-month emergency declared in the Santa Fe Province shown in Fig. 3). Therefore, an index-based drought alert system should be sensitive to an early detection of plant and environmental changes (before yield loss) while not prolonging the alert unnecessarily.

SMADI also showed a non-negligible amount of false positives when considering the spatial extension of different drought classes (53% false positives), but with fewer events showing extreme values (41%). Even so, a distinct sign of the SMADI performance was the large difference between true positives and false positives (31%) and extreme (35%) metrics. The difference in duration was lower (7%), with shorter false positive events than true positive events.

Looking at the whole period, SSMA presented lower detection capabilities for actual events than SMADI, with less than 50% when taking into account the extension of different drought classes and only nine events with extreme values (18%). Furthermore, on average, detected events seemed to be shorter for SSMA than for SMADI. However, for nondrought events, SSMA showed better performance than SMADI, with a low false positive occurrence (24%), only 10% of extreme false positives, and a slightly shorter duration than for actual events. The fact that SSMA showed both a lower % true positives and a lower % false positives does not mean SSMA is more reliable than SMADI, but that it is less sensitive to dry conditions.

This lower sensitivity for drought detection of SSMA as compared to SMADI could be due to at least three factors. First, the spatial resolution of these two indices is very different. ESA-CCI SM Combined product used to calculate SSMA is provided with a pixel of 0.25° by 0.25°, which includes 25 pixels of 0.05° by 0.05° used for SMADI calculation. Second, there is a difference in the reference period used. SSMA is computed with a 40 year baseline period, while SMADI uses the maximum and minimum value of the 5-year studied period. Third, ESA CCI-SM product only represents surface moisture, which does not necessarily reflect changes in root-zone SM that impacts vegetation status, whilst SMADI includes vegetation status in its formulation.

Annually, SSMA exhibited good detection of actual events in 2011–2012 and 2012–2013 (though lower than SMADI), but inferior detection capabilities for 2010–2011 and 2013–2014. Similarly, for nondrought events, the periods 2011–2012 and 2012–2013 showed the largest percentage of false positives both for all drought categories and for extreme values of SSMA, although they are still low values. Interestingly, the difference between years in actual events detection capabilities was not related to the number of observations of ESA-CCI-SM. For instance, 2011–2012 is the year with the largest true positive percentage and with the lowest spatio-temporal coverage (60%, not shown).

Analyzing total values, SPI1 showed a reasonably good agricultural drought detection capability, when considering all drought categories (76%). However, this percentage was considerably reduced (to 35%) when considering the occurrence of extreme values. For nondrought events, SPI1 showed more than 60% false positives when considering all drought categories. This percentage was reduced to 28% if extreme values were requested for considering a drought event. Unfortunately, this led to a small difference between true positive and false positive detection regardless of the request for extreme values or not (less than 10% difference in either case). Moreover, duration scores were low and similar in actual drought and nondrought events with an even smaller difference (1%). As compared with the SMADI results, SPI1 presented lower values in all performance metrics for actual events, a higher percentage of false positives when taking into account all drought classes, and lower values of duration and extreme percentages for nondrought events.

Annually, for actual events, SPI1 showed a very good detection capability (75% or more) except in 2013–2014 when the transition from a dry to a wet period occurred. Particularly, in 2012–2013 most of the detected events included extreme values. For both true and false positives, duration was lower than 20% for all years. For nondrought events, and according to the percentage of false positives, the worst performance was observed in 2011–2012 and 2012–2013, a bad performance was seen for 2010–2011 and 2014–2015 and a moderate performance for 2013–2014 and the second part of 2015.

Compared with SMADI, the duration and extreme percentages of actual events were lower for SPI1 for every year, and even the highest score of SPI1 is lower than the lowest one for SMADI (except for % positive in 2010–2011). For nondrought events, SPI1 also shows lower scores than SMADI (except for % false-positives in 2010 to 2013).

SPI1 and SMADI differences could be due to at least three factors: first, SPI only accounts for precipitation deficit [18], which at a one-month scale does not necessarily propagate to a deficit on SM or plant available water leading to crop failure. For instance, during an intense drought, one month of normal rainfall would lead to a SPI$\sim$0 (and thus would not be included in the duration calculation) but could not be enough to overcome soil dryness and/or vegetation water stress.

Second, as in the SSMA case, SPI is provided at a spatial resolution of 0.25°. Besides that, SPI is computed using precipitation data from meteorological stations that are further apart than 0.25° [17]. Thus, in order to obtain a spatially complete map, point SPI calculations are interpolated with techniques of varying complexity that inevitably add uncertainties to the index.

Third, the temporal resolutions at which SMADI and SPI are computed are different. Even though time conditions for establishing a match are nearly the same (28 days versus a month, respectively), SMADI is computed as an integration of conditions over 14 days. This might be giving SMADI an improved sensitivity, especially at the beginning and end of drought events, over the monthly calculation used for SPI. Still, SPI calculation for shorter periods than a month led to unstable results in a previous study carried out in the same region [17] and therefore was not considered in this work.

As in the SSMA case, there is also a difference in the indices reference period. As it was stated in the methodology section, SPI calculation employed a 40-year reference period (1971–2010), and for SMADI the five years under study are at the same time the reference period. However, this does not explain the obtained results, since a lower sensitivity on SPI for the detection of true positives should affect in the same manner the sensitivity for false positives detection, instead of leading to lower true positives and higher false positives.

SPEI1 exhibited very good detection capabilities of total actual events (82% of positives), in between those from SMADI and from SPI1 though closer to the ones from the former. However, it presented a very high amount of false positives (71%, even worse than SPI1), resulting in only an 11% difference between true and false positives. In both actual and nondrought cases, most of the detected events did not include extreme index values. Duration metric was low and the same for both actual and nondrought events. Compared to SSMA, SPEI1 showed better results for actual events, and worse results for nondrought events for all metrics.

The spatial and temporal resolution, and the reference period are the same for SPI and SPEI. Thus, the improvement on SPEI1 true positives and duration metrics could be due to the fact that SPEI also includes the PET alongside precipitation data. Yet that improvement was not reflected in the nondrought case, where the inclusion of PET led to a worse performance. Still, all SPEI1 scores were far worse than the ones obtained for SMADI, which takes into account information on actual vegetation status and actual SM (instead of considering them indirectly through PET and precipitation respectively).

Even when [17] and [65] state that the three-monthly temporal scale is the most suited to reflect agricultural droughts, our results show a different situation. We can see that SPI3 showed a lower detection ability of actual events than SPI1 ($<$10%) when considering all drought categories and the whole studied period. However, detected events showed a larger average duration, and more of them showed the presence of extreme SPI values. For nondrought events, SPI3 showed a lower % positive and % extreme and a larger duration of detected events than SPI1. This, in turn, led to a smaller difference between true and false positives for SPI3 than for SPI1.

As observed for SPI, SPEI3 did not provide better results than SPEI1. Although SPEI3 showed a lower percentage of false positives than SPEI1, it also had a lower percentage of true positives. This led to a smaller difference between those parameters for SPEI3 than for SPEI1 (7% versus 10%, respectively). Both in the actual events and in the nondrought events, at the three-monthly scale events showed a longer duration and a higher proportion of events with extreme values.

Scaini *et al.* [30] also found a better ability of SPI and SPEI to monitor in situ SM anomalies with shorter time scales (of one month). For time scales longer than 60 days, they found that the response of the indices to SM variability decreased noticeably. Noting there is previous evidence that the use of shorter scales (of less than a month) for SPI and SPEI in Argentina leads to unstable results [17], our results suggest that SM-based indices with a biweekly time scale could be more appropriate than precipitation-based indices to detect agricultural drought in the region.

As a summary of the results, SMADI had the greatest potential to detect agricultural drought events in Argentina, showing a better predictive capability of actual events for the studied period than the other indices, including extreme conditions. SPEI1 and SPI1 followed, particularly as regard to a poor detection of duration and severity. Finally, SPI3, SPEI3, and SMA showed the lowest detection rates. Regarding false positive detection, SMADI was the second best, after SMA.

C. Early Warning System Suitability Analysis

In order to evaluate the suitability of the different studied indices for their use in an early warning system, Table VII gives the results of the five analyzed categorical statistics.

Among the studied indices, SMADI was the one attaining best performance scores, with the best (highest) TPR and F1-score, and the second best FPR (second lowest), PPV (second highest) and OA (second highest). In other words, SMADI outperformed

TABLE VII
CATEGORICAL STATISTICS USED TO EVALUATE THE PERFORMANCE OF THE SIX STUDIED INDICES FOR THE DETECTION OF BOTH ACTUAL DROUGHT AND NONDROUGHT EVENTS

	Target value	SMADI	SSMA	SPI1	SPEI1	SPI3	SPEI3
TPR (%)	100	84	47	76	82	65	73
FPR (%)	0	53	24	63	71	59	66
PPV (%)	100	32	36	26	25	25	24
F1-score (%)	100	46	41	39	38	36	37
OA (%)	100	56	69	45	41	47	43

indices based solely on soil moisture data (SSMA), and those based on precipitation data (SPI), even if they incorporated potential evapotranspiration (SPEI). SMADI also showed the largest difference between TPR and FPR, something that is especially critical for an early warning system because it provides more credibility to the potential warnings, i.e., it makes it more likely that if the warning system states there is a drought, this is accurate, and it is not a false alarm.

SSMA showed the lowest values of both TPR (worst result) and FPR (best result). The large (twofold) difference between TPR and FPR led to SSMA having the largest (best) PPV. This, in turn, compensated the lowest TPR in F1-score calculation, leading to the second best value (second highest) of that metric between the analyzed indices. Furthermore, SSMA illustrated the doubtful utility of OA as a performance metric in imbalanced classifications. In this analysis, the number of nondrought events is over 3 times the number of drought events, and thus, the lowest FPR, which means the largest number of true negatives, resulted on the highest (best) OA, even when SSMA has the lowest TPR, an essential characteristic for any drought detection system.

Precipitation-based indices showed a better performance to detect agricultural droughts at the one-month scale than at the three-month scale, in agreement with [34], and opposed to what was reported in [17] and [65].

The fact that all indices except SSMA showed a large FPR could indicate that within the periods between declared emergencies (that we considered to be nondrought events) there may have occurred some mild droughts, events that were not severe enough as to affect productive activities, or that occurred in moments not critical to productive activities.

To summarize, the indices that include SM information showed a better suitability for an agricultural drought early warning system (with a better performance for SMADI than for SSMA). This should not come as a surprise, since agricultural drought is defined as a deficit of water in the soil unsaturated zone that could compromise the crop yields. Yet our results underline the value of using readily-available satellite-based SM products for early detection of agricultural drought. Precipitation based indices at the monthly scale showed intermediate suitability, and at 3-monthly scale showed lowest suitability, with SPI showing better results than SPEI. While these two indices are generally used for detection of meteorological drought, our results indicate that they may not be as well suited for detection of agricultural drought.

V. CONCLUSION

As a first step to assess their utility in drought early warning systems, we have compared the performance of SMADI, SSMA, SPI and SPEI (these last two with one and three month scales) for the detection of droughts that were severe enough to be declared as "agricultural emergencies." Among them, SMADI showed the best overall performance, with the highest TPR and F1-score, and the second best FPR, PPV, and OA. SMADI also showed the largest difference between TPR and FPR. SSMA showed the lowest FPR, but also the lowest TPR, making it not useful for an alert system. Furthermore, precipitation-based indices, yet simple and widely used, showed not to be suitable indicators for detection of agricultural drought for Argentina, neither in the monthly nor in the three-monthly scale.

Results indicated that the use of SMADI index that explicitly combines SM, LST and vegetation condition data significantly improves drought detection, as compared with indices based only on meteorological data or only on SM data. SMADI is a simple and intuitive index, with good properties for implementation in early warning systems, as shown in this paper. Investigating the development of more advanced models using a wider suite of satellite variables characterizing land surface conditions -such as root-zone SM or vegetation optical depth- is a matter of future research. Such exercise could be helpful to further enhance SMADI capabilities by including new features and encoding (nonlinear) physical mechanisms driving prone-conditions in agroecosystems that may be missed by the current formulation of the index.

ACKNOWLEDGMENT

SPEI and SPI index data is freely available and was downloaded from https://sissa.crc-sas.org/monitoreo/indices-de-sequia/. SMADI global data for the study period was calculated by the authors and shared freely at http://doi.org/10.5281/zenodo.3247649. ESA-CCI products are available through registration at http://www.esa-soilmoisture-cci.org.

REFERENCES

[1] A. Dai, "Increasing drought under global warming in observations and models," *Nature Clim. Change*, vol. 3, no. 1, pp. 52–58, Jan. 2013, doi: 10.1038/nclimate1633.
[2] J. Spinoni, G. Naumann, H. Carrao, P. Barbosa, and J. Vogt, "World drought frequency, duration, and severity for 1951–2010," *Int. J. Climatol.*, vol. 34, no. 8, pp. 2792–2804, Jun. 2014, doi: 10.1002/joc.3875.
[3] J. A. Foley *et al.*, "Solutions for a cultivated planet," *Nature*, vol. 478, no. 7369, pp. 337–342, Oct. 2011, doi: 10.1038/nature10452.
[4] F. N. Kogan, "Monitoring drought from space and food security," in *Remote Sensing for Food Security. Sustainable Development Goals Series*. Cham, Switzerland: Springer. 2019, pp. 75–113, doi: 10.1007/978-3-319-96256-6_5.
[5] D. A. Wilhite, and M. H. Glantz, "Understanding: The drought phenomenon: The role of definitions," *Water Int.*, vol. 10, no. 3, pp. 111–120, Jul. 1985, doi: 10.1080/02508068508686328.
[6] A. Mishra, and V. P. Singh, "A review of drought concepts," *J. Hydrol.*, vol. 391, no. 1-2, pp. 202–216, Sep. 2010, doi: 10.1016/j.jhydrol.2010.07.012.

[7] M. P. Llano, W. Vargas, and G. Naumann, “Climate variability in areas of the world with high production of soya beans and corn: Its relationship to crop yields,” *Meteorol. Appl.*, vol. 19, no. 4, pp. 385–396, Jun. 2011, doi: 10.1002/met.270.

[8] N. Pisani-Claro and D. Miazzo, “El campo argentino en números,” FADA: Fundación Agropecuaria Para El Desarrollo Argentino, Córdoba, Argentina. Nov. 2017. Accessed: Nov. 27, 2020. [Online]. Available: http://agro.unc.edu.ar/∼economia/wp-content/uploads/2018/03/El-campo-argentino-en-n%C3%BAmeros-2017

[9] D. Lema, I. B. Amaro, and I. Pace, “Impacto de la sequía sobre los márgenes brutos esperados de soja y maíz en la región pampeana: ¿En qué situación los aumentos de precios compensarían las pérdidas de rendimientos?,” Instituto de Economía – INTA, Buenos Aires, Argentina, Mar. 2018. Accessed: Oct. 25, 2020. [Online]. Available: https://inta.gob.ar/sites/default/files/inta_cicpes_instdeeconomia_lema_impacto_sequia_margenes_brutos_0.pdf

[10] International Federation of the Red Cross and Red Crescent, and Spanish Red Cross, Argentina: Drought Operation Update No.1. Int. Federation Red Cross Red Crescent Soc., Geneva, Switzerland, 2020. Accessed: Jul. 29, 2020. [Online]. Available: https://reliefweb.int/report/argentina/argentina-drought-mdrar017-operation-update-no

[11] A. C. Ravelo, “Caracterización agroclimática de las sequías extremas en la región pampeana Argentina,” *Rev. Facultad Agronomía*, vol. 20, no. 2, pp. 187–192, 2000. [Online]. Available: http://ri.agro.uba.ar/cgi-bin/library.cgi?a=d&c=rfa&d=2000raveloac

[12] A. C. Ravelo, R. Zanvettor, and W. Da Porta, “Desarrollo de un sistema para la detección, seguimiento y evaluación de las sequías agrícolas en Argentina,” *Revista Argentina de Agrometeorología*, vol. 1, no. 2, pp. 27–34, 2001.

[13] A. C. Ravelo, R. Zanvettor, and P. E. C. Boletta, “Atlas de sequías de la república Argentina,” CREAN: Centro de Relevamiento y Evaluación de Recursos Agrícolas y Naturales, Córdoba, Argentina, Sep. 2014, Accessed: Nov. 19, 2020. [Online]. Available: https://www.crean.unc.edu.ar/files/secciones/Material/Atlas%20de%20las%20Seq%20Arg%2024092014.pdf

[14] L. Serio, P. Martín, and G. Murphy, “Evaluación de una metodología de pronóstico estadístico para la condición hídrica del suelo en la región pampeana Argentina,”*Agriscientia*, vol. 27, no. 1, pp. 11–17, Jun. 2010, doi: 10.31047/1668.298x.v27.n1.2820.

[15] R. E. Zanvettor, and A. C. Ravelo, “Using the SPI to monitor the 1999-2000 drought in northeastern Argentina,” *Drought Netw. News*, vol. 12, no. 3, pp. 3–4, Oct 2000. [Online]. Available: https://digitalcommons.unl.edu/droughtnetnews/108

[16] “Integrated drought management tools and guidelines series 2. World meteorological organization (WMO) and global water partnership (GWP),” 2016. Accessed: Feb. 22, 2021. [Online]. Available: https://www.droughtmanagement.info/literature/GWP_Handbook_of_Drought_Indicators_and_Indices_2016.pdf

[17] G. Podestá, M. Skansi, N. Herrera, and H. Veiga, “Descripción de índices para el monitoreo de sequía meteorológica implementados por el centro regional del clima para el sur de américa del sur,” Serie Reportes Técnicos – Reporte Técnico CRC-SAS-2015-001, 2016. Accessed: Jul. 21, 2020. [Online]. Available: https://www.crc-sas.org/es/content/monitoreo/reporte_sequias.pdf

[18] T. B. McKee, N. J. Doesken, and J. Kleist, “The relationship of drought frequency and duration to time scales,” in *Proc. 8th Conf. Appl. Climatol.*, 1993, pp. 179–184.

[19] S. M. Vicente-Serrano, S. Beguería, and J. I. López-Moreno, “A multiscalar drought index sensitive to global warming: The standardized precipitation evapotranspiration index,” *J. Clim.*, vol. 23, no. 7, pp. 1696–1718, Apr. 2010, doi: 10.1175/2009JCLI2909.1.

[20] J. A. Rivera and O. C. Penalba, “Trends and spatial patterns of drought affected area in southern South America,” *Climate*, vol. 2, no. 4, pp. 264–278, Sep. 2014, doi: 10.3390/cli2040264.

[21] A. Sordo-Ward, M. D. Bejarano, A. Iglesias, V. Asenjo, and L. Garrote, “Analysis of current and future SPEI droughts in the la plata basin based on results from the regional eta climate model,” *Water*, vol. 9, no. 11, Nov. 2017, doi: 10.3390/w9110857.

[22] A. Barella-Ortiz and P. Quintana-Seguí, “Evaluation of drought representation and propagation in regional climate model simulations over Spain,” *Hydrol. Earth Syst. Sci. Discuss.*, vol. 23, pp. 5111–5131, Dec. 2018, doi: 10.5194/hess-2018-603.

[23] T. Hartmann, C. Di Bella, and P. Oricchio, “Assessment of the possible drought impact on farm production in the SE of the province of Buenos Aires, Argentina,” *ISPRS J. Photogramm. Remote Sens.*, vol. 57, no. 4, pp. 281–288, Feb. 2003, doi: 10.1016/S0924-2716(02)00153-3.

[24] R. A. Seiler, F. Kogan, and J. Sullivan, “AVHRR-based vegetation and temperature condition indices for drought detection in Argentina,” *Adv. Space Res.*, vol. 21, no. 3, pp. 481–484, Jun. 1998, doi: 10.1016/S0273-1177(97)00884-3.

[25] R. A. Seiler, F. Kogan, and G. Wei, “Monitoring weather impact and crop yield from NOAA AVHRR data in Argentina,” *Adv. Space Res.*, vol. 26, no. 7, pp. 1177–1185, Jun. 2000, doi: 10.1016/S0273-1177(99)01144-8.

[26] H. Carrão, S. Russo, G. Sepulcre-Canto, and P. Barbosa, “An empirical standardized soil moisture index for agricultural drought assessment from remotely sensed data,” *Int. J. Appl. Earth Observ. Geoinf.*, vol. 48, pp. 74–84, Jun. 2016, doi: 10.1016/j.jag.2015.06.011.

[27] F. Grings *et al.*, “Validation strategies for satellite based soil moisture products over Argentina pampas,” *IEEE J. Sel. Topics Appl. Earth Observ. Remote Sens.*, vol. 8, no. 8, pp. 4094–44105, Aug. 2015, doi: 10.1109/JSTARS.2015.2449237.

[28] J. Martińez-Fernańdez, A. Gonzaĺez-Zamora, N. Sańchez, A. Gumuzzio, and C. M. Herrero-Jimeńez, “Satellite soil moisture for agricultural drought monitoring: Assessment of the SMOS derived soil water deficit index,” *Remote Sens. Environ.*, vol. 177, pp. 277–286, May 2016, doi: 10.1016/j.rse.2016.02.064.

[29] A. Mishra, T. Vu, A. V. Veettil, and D. Entekhabi, “Drought monitoring with soil moisture active passive (SMAP) measurements,” *J. Hydrol.*, vol. 552, pp. 620–632, Sep. 2017, doi: 10.1016/j.jhydrol.2017.07.033.

[30] A. Scaini, N. Sánchez, S. M. Vicente-Serrano, and J. Martínez-Fernández, “SMOS-derived soil moisture anomalies and drought indices: A comparative analysis using in situ measurements,” *Hydrol. Processes*, vol. 29, no. 3, pp. 373–383, Jan. 2015, doi: 10.1002/hyp.10150

[31] J. S. Kimball, L. Jones, K. Jensco, M. He, M. Maneta, and R. Reichle, “SMAP L4 assessment of the US northern plains 2017 flash drought,” in *Proc. IGARSS IEEE Int. Geosci. Remote Sens. Symp.*, Jul. 2019, pp. 5366–5369, doi: 10.1109/IGARSS.2019.8898354.

[32] M. Pablos, A. González-Zamora, J. Martínez-Fernández, and N. Sánchez, “Assessment of root zone soil moisture estimations from SMAP, SMOS and MODIS observations,” *Remote Sens.*, vol. 10, no. 7: 981, pp. 1–20. Jun. 2018, doi: 10.3390/rs10070981

[33] M. Pablos, A. González-Zamora, N. Sánchez, and J. Martínez-Fernández, “Assessment of SMADI and SWDI agricultural drought indices using remotely sensed root zone soil moisture,” in *Proc. Int. Assoc. Hydrol.*, Dec. 2018, vol. 380, pp. 55–66, doi: 10.5194/piahs-380-55-2018.

[34] N. Sánchez, A. González-Zamora, M. Piles, and J. M. Fernández, “A new soil moisture agricultural drought index (SMADI) integrating MODIS and SMOS products: A case of study over the Iberian peninsula,” *Remote Sens.*, vol. 8, no. 4: 287, pp. 1–25, Mar. 2016, doi: 10.3390/rs8040287.

[35] N. Sánchez, J. Martínez-Fernández, and A. González-Zamora, “A combined approach with SMOS and MODIS to monitor agricultural drought,” *Int. Arch. Photogramm. Remote Sens. Spat. Inf. Sci.*, vol. XLI-B8, pp. 393–398, Jun. 2016, doi: 10.5194/isprsarchives-XLI-B8-393-2016.

[36] M. Pablos, J. Martínez-Fernández, N. Sánchez, and A. González-Zamora, “Temporal and spatial comparison of agricultural drought indices from moderate resolution satellite soil moisture data over northwest Spain,” *Remote Sens.*, vol. 9, no. 11, Nov. 2017, doi: 10.3390/rs9111168.

[37] N. Sánchez, A. González-Zamora, J. Martínez-Fernández, M. Piles, and M. Pablos, “Integrated remote sensing approach to global agricultural drought monitoring,” *Agricultural Forest Meteorol.*, vol. 259, pp. 141–153, Sep. 2018, doi: 10.1016/j.agrformet.2018.04.022.

[38] *Ministerio de Agricultura*, Ganadería y Pesca (MAGyP), Oficina de Monitoreo de Emergencias y Desastres Agropecuarios (Ministry for Agriculture, Cattle Raising and Fishing, Office for the Monitoring of Agricultural Emergencies and Disasters), Accessed: Oct. 21, 2019. [Online]. Available: https://www.agroindustria.gob.ar/sitio/areas/d_eda/resoluciones/

[39] National Geographic Institute, Madrid, Spain, Accessed: Nov. 19, 2020. [Online]. Available: https://www.ign.gob.ar/NuestrasActividades/Geografia/DatosArgentina/LimitesSuperficiesyPuntosExtremos

[40] National Meteorological Service, Accessed: Aug. 21, 2020. [Online]. Available: https://www.smn.gob.ar/clima/atlasclimatico

[41] Secretaría de Ambiente y Desarrollo Sustentable de la Nación,“Cambio climático en Argentina: Tendencias y proyecciones,” Tercera Comunicación Nacional Sobre Cambio Climático, Buenos Aires, Argentina, 2014, [Online]. Available: https://www.argentina.gob.ar/ambiente/cambio-climatico/tercera-comunicacion/3com.-resumen-ejecutivo-de-la-tercera-comunicacion-nacional.pdf

[42] V. R. Barros, J. A. Boninsegna, I. A. Camilloni, M. Chidiak, G. O. Magrín, and M. Rusticucci, “Climate change in Argentina: Trends, projections, impacts and adaptation,” *WIREs Clim. Change*, vol. 6, pp. 151–169, 2015, [Online]. Available: https://doi.org/10.1002/wcc.316

[43] J. M. Paruelo, A. Beltran, E. Jobbagy, O. E. Sala, and R. A. Golluscio, "The climate of patagonia: General patterns and controls on biotic processes," *Ecologia Austral*, vol. 8, no. 2, pp. 85–101, 1998.

[44] Instituto Nacional de Estadística y Censos. Censo Nacional Agropecuario resultados preliminaries. 1a ed. - Ciudad Autónoma de Buenos Aires. INDEC, 2018, [Online]. Available: https://www.indec.gob.ar/ftp/cuadros/economia/cna2018_resultados_preliminares.pdf

[45] O. Thomasz, A. Vilker, and G. Rondinone, "The economic cost of extreme and severe droughts in soybean production in Argentina," *Contaduría Y Administración*, vol. 64, no. 1, pp. 1–24, Mar. 2019, doi: 10.22201/fca.24488410e.2018.1422.

[46] Instituto Nacional de Tecnología Agropecuaria (INTA) (National Agricultural Technology Institute, Comodoro Rivadavia, Argentina, *Principales Cultivos Por Provincia Argentina, y Mes De Siembra y Cosecha*, Accessed: Feb. 22, 2021. [Online]. Available: https://inta.gob.ar/documentos/principales-cultivos-por-provincia-argentina-y-mes-de-siembra-y-cosecha

[47] "Dirección nacional de agricultura - Dirección de estimaciones agrícolas," Ministerio de Agricultura, Ganadería y Pesca (MAGyP), Accessed: Mar. 1, 2021. [Online]. Available: http://datosestimaciones.magyp.gob.ar/reportes.php?reporte=Estimaciones

[48] T. N. Carlson, R. R. Gillies, and E. M. Perry, "A method to make use of thermal infrared temperature and NDVI measurements to infer surface soil water content and fractional vegetation cover," *Remote Sens. Rev.*, vol. 9, no. 1/2, pp. 161–173, Mar. 1994, doi: 10.1080/02757259409532220.

[49] G. Petropoulos, T. N. Carlson, M. J. Wooster, and S. A. Islam, "Review of TS/VI remote sensing based methods for the retrieval of land surface energy fluxes and soil surface moisture," *Prog. Phys. Geography,* vol. 33, no. 2, pp. 224–250, Jun. 2009, doi: 10.1177/0309133309338997.

[50] I. Sandholt, K. Rasmussen, and J. Andersen, "A simple interpretation of the surface temperature/vegetation index space for assessment of surface moisture status," *Remote Sens. Environ.*, vol. 79, no. 2/3, pp. 213–224, Feb. 2002, doi: 10.1016/S0034-4257(01)00274-7.

[51] C. Xu *et al.*, "Downscaling of surface soil moisture retrieval by combining MODIS/Landsat and in situ measurements," *Remote Sens.,* vol. 10, no. 2: 210, pp. 1–16, Feb. 2018, doi: 10.3390/rs10020210.

[52] M. Piles *et al.*, "Downscaling SMOS-derived soil moisture using MODIS visible/infrared data," *IEEE Trans. Geosci. Remote Sens.*, vol. 49, no. 9, pp. 352–374, Sep. 2011, doi: 10.1109/TGRS.2011.2120615.

[53] M. Piles, G. Petropoulos, N. Sánchez, A. González- Zamora, and G. Ireland, "Towards improved spatio-temporal resolution soil moisture retrievals from the synergy of SMOS and MSG SEVIRI spaceborne observations," *Remote Sens. Environ.*, vol. 180, pp. 403–417, Jul. 2016, doi: 10.1016/j.rse.2016.02.048.

[54] G. Portal *et al.*, "A spatially consistent downscaling approach for SMOS using an adaptive moving window," *IEEE J. Sel. Topics Appl. Earth Observ. Remote Sens.*, vol. 11, no. 6, pp. 1883–1894, Jun. 2018, doi: 10.1109/JSTARS.2018.2832447.

[55] F. N. Kogan, "Remote sensing of weather impacts on vegetation in non-homogeneous areas," *Int. J. Remote Sens.*, vol. 11, no. 8, pp. 1405−1419, Aug. 1990, doi: 10.1080/01431169008955102.

[56] F. N. Kogan, "Application of vegetation index and brightness temperature for drought detection," *Adv. Space Res.*, vol. 15, no. 11, pp. 91–100, Nov. 1995, doi: 10.1016/0273-1177(95)00079-T.

[57] S. Park, J. J. Feddema, and S. L. Egbert, "Impacts of hydrologic soil properties on drought detection with MODIS thermal data," *Remote Sens. Environ.*, vol. 89, no. 1, pp. 53–62, Jan. 2004, doi: 10.1016/j.rse.2003.10.003.

[58] F. Zhang, L. W. Zhang, X. Z. Wang, and J. F. Hung, "Detecting agro-droughts in southwest of China using MODIS satellite data," *J. Integr. Agriculture*, vol. 12, no. 1, pp. 159–168, Jan. 2013, doi: 10.1016/S2095-3119(13)60216-6.

[59] M. Pablos, M. Piles, and C. González-Haro, "BEC-SMOS-0003-PD-Land, products description, BEC 2019-7-31. Issue 1.0," Barcelona Expert Center Team, Jul. 2019. Accessed: Nov. 19, 2020. [Online]. Available: http://bec.icm.csic.es/doc/BEC-SMOS-0003-PDLand.pdf

[60] A. González-Zamora, N. Sánchez, and M. Piles, Global Soil Moisture Agricultural Drought Index (SMADI) (Version 1.0.0), Zenodo, Genève, Switzerland, 2019. [Online]. Available: http://doi.org/10.5281/zenodo.3247649

[61] W. A. Dorigo *et al.*, "ESA CCI soil moisture for improved earth system understanding: State-of-the art and future directions," *Remote Sens. Environ.*, vol. 203, pp. 185–215, Dec. 2017, doi: 10.1016/j.rse.2017.07.001.

[62] A. Gruber, W. A. Dorigo, W. Crow, and W. Wagner, "Triple collocation-based merging of satellite soil moisture retrievals," *IEEE Trans Geosci Remote Sens.*, vol. 55, no. 12, pp. 6780–6792, Sep. 2017, doi: 10.1109/TGRS.2017.2734070.

[63] A. Gruber, T. Scanlon, R. van der Schalie, W. Wagner, and W. Dorigo, "Evolution of the ESA CCI soil moisture climate data records and their underlying merging methodology," *Earth Syst. Sci. Data*, vol. 11, no. 2, pp. 717–739, May 2019, doi: 10.5194/essd-11-717-2019.

[64] European Drought Observatory, Soil Moisture Anomaly factsheet, 2019. Accessed: Sep. 1, 2020. [Online]. Available: https://edo.jrc.ec.europa.eu/documents/factsheets/factsheet_soilmoisture.pdf

[65] L. C. Sgroi, M. A. Lovino, E. H. Berbery, and G. V. Müller, "Characteristics of droughts in Argentina's core crop region," *Hydrol. Earth Syst. Sci.*, vol. 25, pp. 2475–2490, 2021.

[66] Sistema de Información sobre Sequías para el sur de Sudamérica, Centro Regional del Clima para el Sur de América del Sur, CRC-SAS, 2020. (Drought Information System for the South of South America, Regional Climate Center Network for Southern South America). 2020. Accessed: Jul. 7, 2020. [Online]. Available: https://sissa.crc-sas.org/monitoreo/indices-de-sequia/

[67] Standardized Precipitation Index User, World meteorological organization, 2012. Geneva, Switzerland. Accessed: Aug. 3, 2020. [Online]. Available: http://library.wmo.int/index.php?lvl=notice_display&id=13682#.XyhnqChKjIU

[68] J. L. McBride and E. E. Ebert, "Verification of quantitative precipitation forecasts from operational numerical weather prediction models over australia," *Weather Forecasting*, vol. 15, no. 1, pp. 103–121, Feb. 2000, doi: 10.1175/1520-0434(2000)015<0103:VOQPFF>2.0.CO;2.

[69] D. M. W. Powers, "Evaluation: From precision, recall and F-Score to ROC, informedness, markedness & correlation," *J. Mach. Learn. Technol.*, vol. 2, no. 1, pp. 37–63, 2011, doi: 10.9735/2229-3981 , [Online]. Available: https://arxiv.org/abs/2010.16061v1.

[70] C. Toté, D. Patricio, H. Boogaard, R. van der Wijngaart, E. Tarnavsky, and C. Funk, "Evaluation of satellite rainfall estimates for drought and flood monitoring in mozambique," *Remote Sens.,* vol. 7, no. 2, pp. 1758–11776, Feb. 2015, doi: 10.3390/rs70201758.

[71] A. Ali, S. M. Shamsuddin, and A. L. Ralescu, "Classification with class imbalance problem: A review," *Int. J. Adv. Soft. Comput. Appl.*, vol. 7, no. 3, pp. 176–204, 2015.

[72] L. A. Jeni, J. F. Cohn, and F. De La Torre, "Facing imbalanced data–recommendations for the use of performance metrics," in *Proc. Hum. Assoc. Conf. Affect. Comput. Intell. Interact.*, 2013, pp. 245–251, doi: 10.1109/ACII.2013.47.

M. Mercedes Salvia (Member, IEEE) was born in Buenos Aires, Argentina, in 1980. She received the B.S. and M.S., and Ph.D. degrees in biological science from the Universidad de Buenos Aires, Ciudad Autónoma de Buenos Aires, Argentina on 2004 and 2010, respectively.

From 2010 to 2012, she was a Posdoctoral Fellow, from 2012 to 2015 was an Assistant Researcher, and since 2015, she has been an Associate Researcher with the Quantitative Remote Sensing Group, Institute for Astronomy and Space Physics, IAFE (CONICET-UBA). Her research interests include the analysis of temporal series of optical and microwave satellite images and derived products to study wetland dynamics, forests, and climate, including hydrological extreme events.

Dr. Salvia has been a member of the IEEE Argentina Geoscience and Remote Sensing Society Chapter since 2015, and was the chapter's Vice-President from 2016 to early 2021.

Nilda Sánchez was born in Cordoba, Spain. She received the M.Sc. and Ph.D. degrees in cartographic engineering from the University of Salamanca (USAL), Salamanca, Spain, in 2002 and 2009, respectively, and the M.S. degree in geographical information systems from the University of Girona, Girona, Spain, in 2000.

Since 1994, she has been an Associate Professor with USAL. She has participated and conducted several national and international research programs under the Spanish Ministry of Science and Research, the European Space Agency and the European Commission. She is with the Water Resources Research Group (HIDRUS), Instituto Hispano-Luso de Investigaciones Agrarias, USAL. Her activities in this group are devoted to hydrological and agricultural applied research supported by remote sensing. Her research interests include the estimation of soil moisture and vegetation characteristics as well as applications based in satellite imagery such as agricultural drought and crop monitoring.

María Piles (Senior Member, IEEE) received the B.Sc. degree in telecommunication engineering from the Universitat Politècnica de València, València, Spain, in 2005, and the Ph.D. degree in signal theory and communications from the Universitat Politècnica de Catalunya (UPC), Barcelona, Spain, in 2010.

She was a Research Fellow with the University of Melbourne, Melbourne, VIC, Australia, in 2010, and a Research Scientist with UPC, from 2011 to 2016, associated with Massachusetts Institute of Technology, Cambridge, MA, USA. In 2016, she was a Research Scientist with the Institute of Marine Sciences from the Spanish National Research Council. Since 2017, she has been a Ramón y Cajal Senior Researcher with the Imaging Processing Laboratory, Universitat de València, València, Spain. She has been actively involved in the scientific activities of the two first space missions dedicated to measuring the Earth's soil moisture, European Space Agency (ESA's) SMOS and NASA's SMAP. He is a Member of the Mission Advisory Group of the CIMR High Priority Copernicus Mission. She has authored or coauthored 62 articles in international peer-reviewed journals, four book chapters and more than 1000 international conference papers. Her research activity is centered in microwave remote sensing, retrieval of land biogeophysical parameters and development of multisensor synergistic techniques for applications of ecology, agriculture, forest conservation and a better understanding of earth system processes.

Dr. Piles is currently the President of the IEEE Spain Geoscience and Remote Sensing Society (GRSS) Chapter.

Romina C. Ruscica was born in Buenos Aires, Argentina in 1980. She received the B.S/M.S degree in physics and the Ph.D. degree in atmospheric sciences from the University of Buenos Aires, Buenos Aires, Argentina, in 2009 and 2015, respectively.

From 2015 to 2016, she was a Postdoctoral Fellow; and since 2016, she has been a Research Assistant with the Research Center for the Sea and the Atmosphere "CIMA" (UBA-CONICET-UMIIFAECI3351-CNRS-IRD), Buenos Aires, Argentina. She is an author of 25 research papers, 31 presentations at different meetings and participated in 14 research and development projects. Her research interests include South America climate, land-atmosphere interactions, climate modeling, EO satellite estimates, water cycle processes and climate uncertainty.

Angel González-Zamora was born in Salamanca, Spain, in 1984. He received the B.S. degree in physics and the Ph.D. degree in applied physics and technology from the University of Salamanca, Salamanca, Spain, in 2011, and the M.S. degree in geophysics and meteorology from the Complutense University of Madrid, Madrid, Spain, in 2012.

He is working on hydrologic and agricultural applications of remote sensing with the Instituto Hispano-Luso de Investigaciones Agrarias, Universidad de Salamanca.

Esteban Roitberg was born in Buenos Aires, Argentina, in 1988. He received the B.S. degree in physics in 2016 from the University of Buenos Aires, Buenos Aires, Argentina, where he is currently working toward the Ph.D. degree in physics, working on methods for the detection of deforestation in near-real time in the Chaco Forest.

His research interest includes time series analysis, machine learning and forest conservation.

José Martínez-Fernández was born in Moratalla, Spain, in 1961. He received the B.S. and Ph.D. degrees in physical geography and the M.S. degree in water science and technology from the Universidad de Murcia (UM), Murcia, Spain, in 1985, 1992, and 1991, respectively.

He was a Research Fellow (1988–1992) and a Junior Researcher (1992–1994) with the Department of Geography, UM. He was an Assistant Professor (1995) and an Associate Professor (1997) with the Department of Geography, Universidad de Salamanca (USAL), Salamanca, Spain, where he has been a Professor of physical geography since May 2018. He is currently the Principal Investigator (PI) with the Water Resources Research Group, Instituto Hispano Luso de Investigaciones Agrarias, USAL. He has been PI in twenty four national and international (Regional and Spanish Research Programmes, European Union, European Space Agency) research projects and collaborator in 12. He has been a Member of the Spanish National Biodiversity, Earth Sciences and Global Change Programme R&D Projects Selection Committee. He is author or co-author of 211 publications.